

Structural, Photocatalytic and Antibacterial Activity of ZnO and ZrO₂ Doped ZnO Nanoparticles

Sohair Abd El Hakam¹, Shady Mohamed El-Dafrawy^{2*}, Salah Fawzy³, Shawky Mohamed Hassan⁴

Chemistry Department, Faculty of Science, Mansoura University, Egypt

Abstract: A series of ZnO and ZrO₂ doped ZnO catalysts were prepared by sol-gel method. X-ray diffraction analysis of these catalysts showed the formation of phase pure nanoparticles with wurtzite ZnO structure. Scanning electron microscope (SEM) images emphasized the formation of spherical shaped ZnO and ZrO₂ doped ZnO nanoparticles. Transmission electron microscope (TEM) images emphasized that all prepared catalysts are in nanoscale and are spherically shaped. The Methylene Blue (MB) decomposition rate of the synthesized pure ZnO and ZrO₂ doped ZnO nanoparticles were studied under the UV-Vis region. In the UV-Vis region, synthesized pure ZnO and ZrO₂ doped ZnO decomposed Methylene Blue (MB). However, the MB decomposition rate obtained using pure ZnO was much higher than that by doped ZnO. The antibacterial property test was carried out via disk diffusion method, and the result indicated antibacterial activity of the prepared catalysts.

Keywords: ZnO, Sol-gel, photocatalysis, antimicrobial, ZnO /ZrO₂

1. Introduction

Dyes and organic compounds are widely used in industry and daily life. Large amounts of these compounds were released in waste water resulting in considerable problems to microorganisms, aquatic environments and human beings [1-3]. Unfortunately, most of these dyes are chemically stable and cannot be removed by chemical oxidation via traditional biochemical and physicochemical methods used widely [4-6]. Additionally, traditional methods used widely like chlorination, generates carcinogenic and mutagenic by products [7].

Recently, heterogeneous photocatalysis is investigated widely to replace traditional methods because of its ability to completely decompose targeted pollutants including dyes and organic compounds besides inactivating microorganisms such as bacteria and viruses [1, 6-9].

ZnO is a semiconductor material with a wide band gap (3.2eV) [10], low cost, abundant in nature and environmental friendly so it worth to be studied as one of the most promising materials capable of achieving green chemistry [11-13].

As a heterogeneous photocatalyst, ZnO has comparable band gap with TiO₂ (3.2eV) [14-15], lower productivity cost [16-18], larger quantum efficiency than TiO₂ [19-20] so it absorbs over larger fraction of the solar spectrum than TiO₂ [21-28]. Although ZnO and TiO₂ have similar band gaps, ZnO has higher photoactivity (by a factor of 2 – 3) in both UV and sunlight irradiation for the decontamination of water [29-35]. This is due to the higher efficiency of ZnO in the production of OH⁻ and reduced recombination of photo induced electron-hole pairs [16-18, 36-41].

Point defects mainly from oxygen vacancies are the main reason for the higher efficiency of ZnO in the production of OH⁻ and reduced recombination of photo induced electron-hole pairs [42-46].

The heterogeneous photocatalytic process is initiated when a semiconductor material such as ZnO or TiO₂ is

illuminated with photons possess energy equal or greater than the bending energy of electrons in the valence band, resulting in the generation of mobile electrons in the higher energy conduction band (E_{cb}) and positive holes in the lower energy valence band (E_{vb}) of the catalyst [47].

The photocatalytic reaction depends on holes formed in the valence band which catalyze formation of hydroxyl radicals at the semiconductor surface and mobile electrons in the conduction band which reduce molecular O₂. These reactions represent steps to both mineralization of organic species and removal of inorganic cations [48-51].

In this work, we aimed to synthesize nontoxic, environmental friendly and affordable photocatalyst to investigate in the removal of MB as a well-known water pollutant. MB is a heterocyclic organic dye, frequently used in textile, cosmetic and pharmaceutical industries. MB can cause permanent injury to humans and animals on inhalation and ingestion and the risk of the presence of this dye in water may be arisen from the burning effect of eye, nausea, vomiting and diarrhea [52]. Moreover, we studied the antimicrobial activity of ZnO and ZrO₂ doped ZnO against gram positive and gram negative bacteria.

2. Experimental

2.1. Preparation of Catalysts:

2.1.1. Zinc Oxide nanoparticles synthesis:

Zinc Oxide nanoparticles were prepared by sol-gel method from zinc acetate dihydrate and oxalic acid using ethanol as solvent [53-54]. ZnO gel was obtained by dissolving 10.99g zinc acetate dihydrate in 300ml ethanol (C₂H₆O) and refluxing for 30 minutes. 17.71g oxalic acid (H₂C₂O₄) was mixed with 200ml of ethanol; stirred for 1 hr at 50 °C and added to the previous solution slowly. The final mixture was refluxed at 50 °C for 60 minutes before left cool down to room temperature. Finally, the prepared ZnO gel was dried at 80 °C for 20 hrs (xerogel), and the powder calcined under flowing air (0.1mmolS⁻¹) for 3 hrs at (400,500 and 600 °C).

2.1.2. ZrO₂ doped zinc oxide Synthesis:

Zirconium nitrate was dissolved in ethanol and added to ZnO gel, stirred for 1 hr, dried at 80 °C for 20 hrs to form xerogel and finally calcined at 500 °C to synthesize 0.005, 0.01, 0.015 and 0.02 ZrO₂/ZnO molar ratios.

1.2. Characterization of catalysts:

XRD was used to determine the nature and the size of crystalline phases of ZnO and ZrO₂ doped ZnO. Patterns were obtained with hand pressed samples mounted on a Philips PW 1830 goniometer using the Cu K_α line ($\lambda = 0.15458$ nm) radiation under 40 kV and 100 mA and scanning with the 2θ ranging from 10° to 70° [54].

ZnO and ZrO₂ doped ZnO particles sizes were examined by a Jeol JSM-840 scanning electron microscope (SEM) under high vacuum and acceleration voltage of 200 KeV. The samples were deposited onto carbon tape and coated with gold in a Blazers plasma sputterer (30s at 30mA).

Particle size and shape of nano ZnO and ZrO₂ doped ZnO particles were examined by JEM-2100F transmission electron microscope (TEM) at a voltage of 300 KeV. Transmission electron micrograph gives directly the size and shape distributions. The powders are dispersed in Ethanol by stirring in an ultrasonic tank for 15 min. A drop of this suspension was then mounted on a carbon-coated copper grid for analysis [41].

The total acidity of all catalysts was determined by means of the potentiometric titration method using an Orion 420 digital model using a double junction electrode. In this method, 0.1gm catalyst was heated under vacuum, and then 10 ml of acetonitrile was added. After agitation for 2hrs, the suspension was titrated by 0.01N N-butyl amine in acetonitrile. The addition is continued till no further change of mV recorded [55].

Photocatalytic activity measurements of ZnO and 0.005M ZrO₂/ZnO powders were evaluated by measuring the degradation of MB in water under the UV/Vis light. The MB degradation was carried out at 20 °C with external lamp (400w UV/Vis lamps, Halogen Mercury lamp).

The amount of catalyst powder [ZnO] was kept at 1g.L⁻¹, the initial concentration of MB, C₀, was 10mgL⁻¹, and the pH of the solution was fixed to 7.

Photoactivity experiments were realized with varying operating variables: three different pH values (2.5, 7 and 10) adjusted with aqueous solution of HCl and NaOH and four initial concentrations of MB, C₀ (10, 20, 50 and 100 mgL⁻¹).

Before each photocatalytic test, the mixture was kept in the dark for 30 minutes to ensure that the adsorption-desorption equilibrium was reached before illumination. The sample was then taken out at the end of the dark adsorption period, just before the light was turned on, in order to determine MB concentration in solution, C₀.

The experiment starts by turning on the lamp. After a given irradiation time sample was taken, centrifuged and the MB photodegradation monitoring was performed on a Shimadzu, MPC-2200 UV-Vis spectrophotometer [53].

Antimicrobial activity of heterogeneous catalysts was tested against a panel of gram positive staphylococcus Aureus and gram negative candida Albicans. Each of the catalysts was dissolved in DMSO and solution of the concentration 1mg/ml was prepared separately. Paper discs of walt man filter paper were prepared with standard size (5cm), were cut and sterilized in an autoclave.

The paper discs soaked in the desired concentration of the complex solution were placed aseptically in the petridishes containing nutrient agar media (agar 20g + beef extract 3g + peptone 5g) and seeded with staphylococcus aureus or candida Albicans. The petridishes were incubated at 36 °C and the inhibition zone were recorded after 24hrs of incubation. Each treatment was replicated three times. The antibacterial activity of a common standard antibiotic ampicillin and antifungal colitrimazole was also recorded using the same procedure as above at the same concentration and solvents [56]. The % activity index for the complex was calculated by the following formula:

$$\% \text{activity index} = \frac{\text{Zone of inhibition by test compound (diameter)}}{\text{Zone of inhibition by standard (diameter)}} \times 100$$

3. Results and Discussion**3.1. XRD Analysis:**

The XRD patterns of prepared samples are shown in Fig.1. The sharp and intense peaks indicate that ZnO and ZrO₂ doped ZnO samples are highly crystalline. All of the indexed peaks indicate that all the samples are the typical wurtzite hexagonal structure (JCPDS card No.36-1451) [57]. No phases for ZrO₂ were observed. The intensity of (101) and (002) peaks increases with increasing ZrO₂ content because the ionic radius of Zr⁴⁺ (0.84 Å) is larger than that of Zn²⁺ (0.74 Å). Consequently, the more Zn²⁺ ions are substituted by Zr⁴⁺, the more lattice expansion occurs and ZnO particles become larger [58-59]. These results indicate that the Zr atoms have entered into the ZnO lattices instead of forming other lattices.

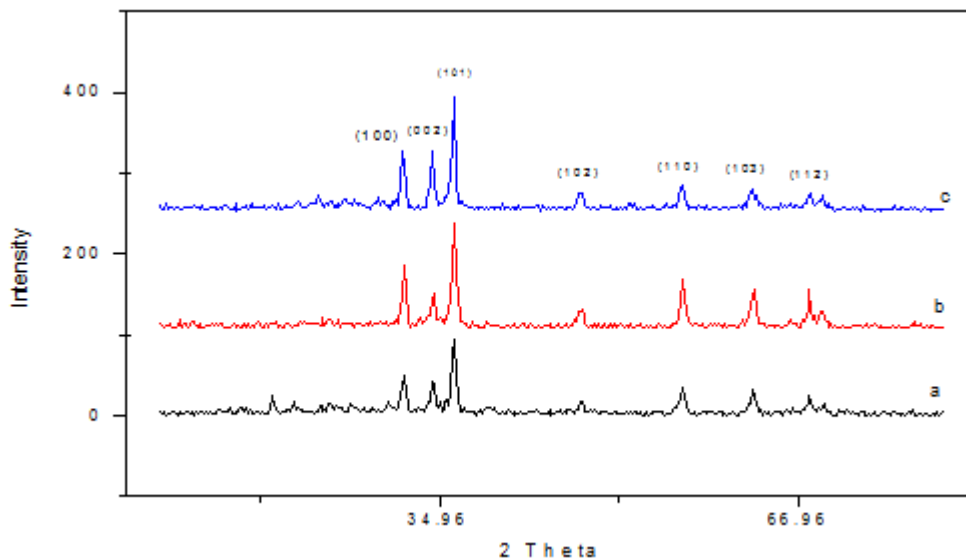
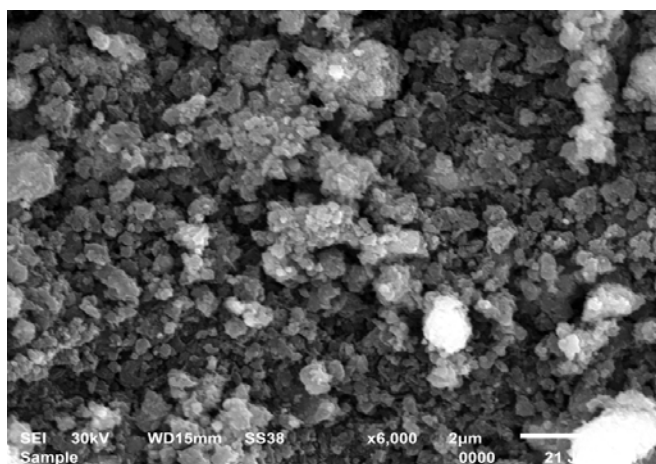


Figure 1: XRD pattern of (a) ZnO, (b) 0.01M ZrO₂/ZnO, (c) 0.02M ZrO₂/ZnO

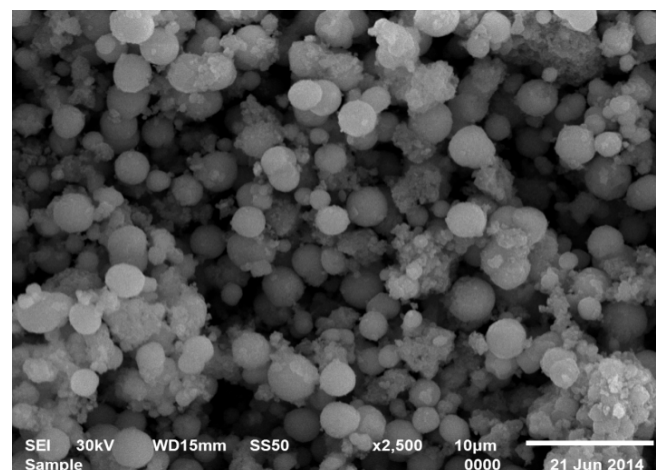
3.2. SEM Analysis:

The surface morphology of the prepared catalysts was examined by SEM analysis. The SEM images show that the particles to some extent are aggregated. Fig.2(I) shows that ZnO has irregular spherical shape. However, in Fig.2(II, III) The SEM micrographs of the 0.01M ZrO₂/ZnO and 0.02M ZrO₂/ZnO appear in spherical shape perfectly. Fig.2 shows also that ZnO and ZrO₂/ZnO nanoparticles have particle size ranging between 90 to 150nm.

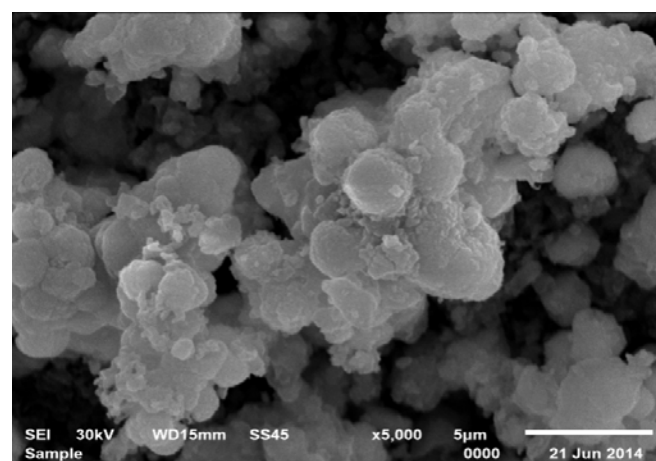
The difference in the particle sizes shown by XRD and SEM analysis for ZnO and ZrO₂ doped ZnO could be due to particles aggregation [57]. In addition, the SEM measurements are based on the difference between the visible grain boundaries, while XRD calculations measure the extended crystalline region that diffracts X-ray coherently. Hence, XRD method has more straight criterion and leads to smaller sizes [60].



I



II



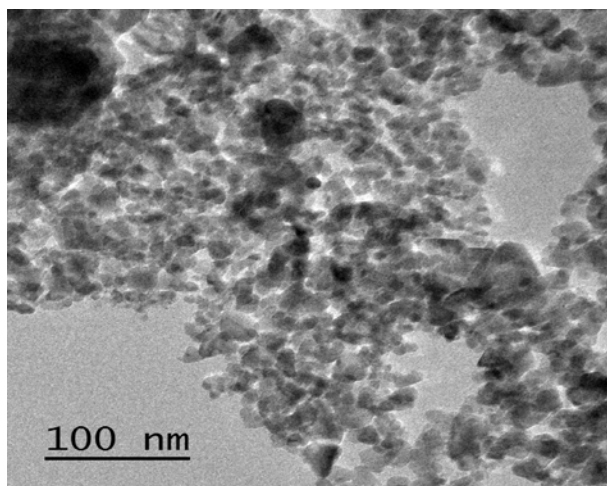
III

Figure 2: SEM images of (I) ZnO, (II) 0.01M ZrO₂/ZnO and (III) 0.02M ZrO₂/ZnO

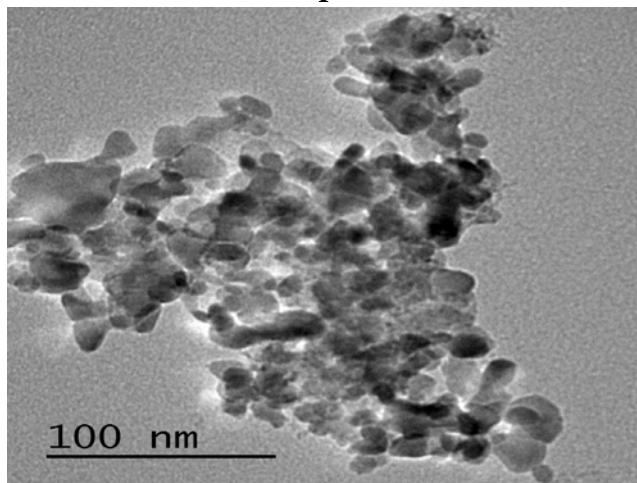
3.3. TEM analysis:

Figure 3 TEM images illustrate ZnO and ZrO₂/ZnO nanoparticles are almost hexagonal (spherical) in shape and are agglomerated up to some extent. The average

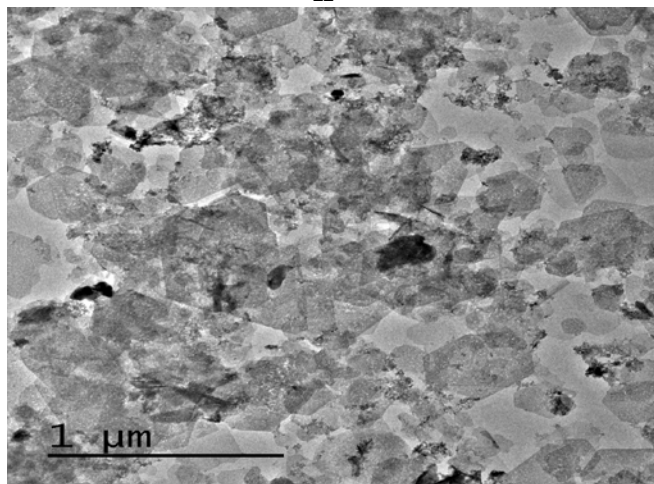
nanoparticles diameter measured of ZnO is < 25nm as shown in Fig. 3 (I) .The particles size increases with increasing ZrO₂ content. Fig.3 (II) shows that when ZrO₂ content increased to 0.01M ZrO₂/ZnO a slight increase in grain size is observed, however, when it increases to 0.02M ZrO₂, the grain size increases sharply to about 0.2 μm as shown in Fig.3 (III). Consequently, TEM results illustrated in Fig.3 roughly agrees with XRD shown in Fig.1 in that ZnO crystal size increases by increasing ZrO₂ content.



I



II



III

Figure 3: TEM images of (I) ZnO, (II) 0.01M ZrO₂/ZnO and (III) 0.02M ZrO₂/ZnO

3.4. Acidity test:

The surface acidity of the investigated catalysts was determined by non-aqueous titration of n-butyl amine (PK_a=10.73), which is a basic molecule suitable for titrating the medium and strong acid sites on the surface of the investigated catalysts. Fig.4: illustrates the variation of the electrode potential for the investigated catalysts calcined at 500 °C with volume added from n-butyl amine. This figure shows that, as the acid sites of the solid become neutralized, a buffer behavior becomes more apparent. The trend of the titration curve is asymptotic, leading to a characteristic value on the potential (mV) axis [55]. This is related to the volume added from n-butyl amine / g needed for neutralization of the surface acidity. The magnitude of change of the electrode potential in this method is related to the surface acidity of the catalyst. Table 1: shows the volume of n-butyl amine /g needed for the neutralization of the surface acidity of catalysts as a function of ZrO₂ content and the total number of acid sites/g. This technique was carried out by measuring the electrode potential (mV) as a function of the progressive increase of the n-butyl amine concentration expressed as (mmol n-butyl amine / g catalyst) [55]. The total number of acid sites / g of the catalysts were calculated from the following relation:

$$\text{Total number of acid sites / g} = (\text{ml equivalent / g}) \times N \times 1000$$

(Where N is Avogadro's number).

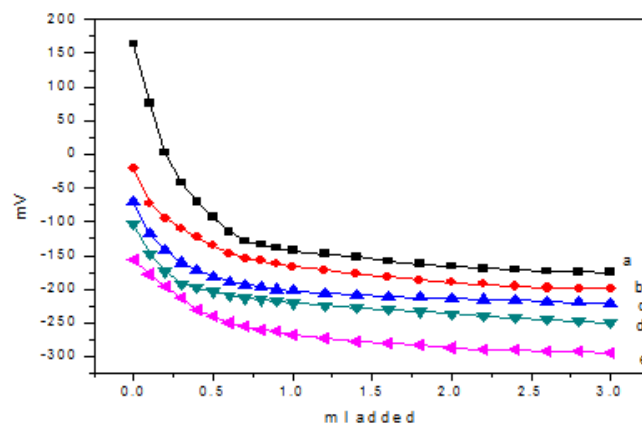


Figure 4: Acidity curves for (a) ZnO, (b) 0.005M ZrO₂/ZnO, (c) 0.01M ZrO₂/ZnO, (d) 0.015M ZrO₂/ZnO, (e) 0.02M ZrO₂/ZnO

Table 1: Volumes of n-butyl amine/g and total number of acid sites/g

Sample	ml added	Total No of acid sites/g
ZnO	0.35	2.1×10 ¹⁹
0.005M ZrO ₂ /ZnO	0.30	1.81×10 ¹⁹
0.01M ZrO ₂ /ZnO	0.266	1.6×10 ¹⁹
0.015M ZrO ₂ /ZnO	0.25	1.5×10 ¹⁹
0.02M ZrO ₂ /ZnO	0.23	1.38×10 ¹⁹

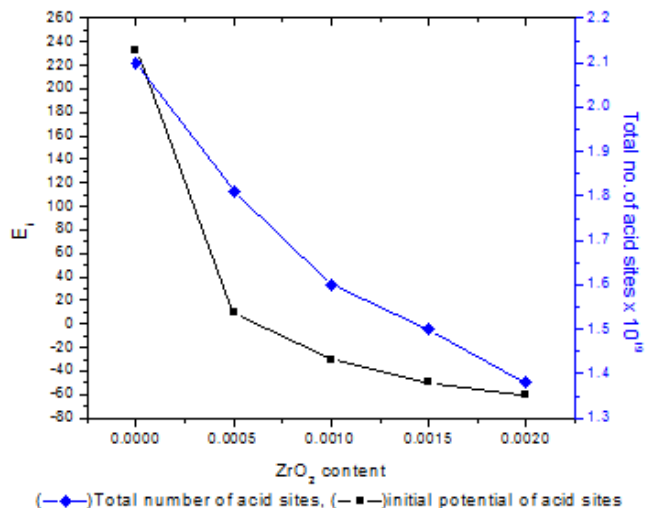


Figure 5: Effect of ZrO₂ content on total number of acid sites and initial potential of acid sites

3.5. Photocatalytic Activity:

The photocatalytic activity of ZnO and ZrO₂ doped ZnO was investigated using MB Dye. MB was irradiated under UV-Vis light in absence of catalyst (photolysis), in absence of light (adsorption) and under UV-Vis light in presence of catalyst (photocatalysis). The results of the studies are illustrated in Fig.6. It is observed that direct photolysis did not cause any significant degradation in absence of catalyst. In the presence of ZnO without irradiation, MB showed a slight adsorption on ZnO surface but no degradation occurred. Irradiation of MB under UV-Vis light caused 99% degradation in 60 min. The photodegradation leads to the conversion of organic carbon into harmless gaseous CO₂ and that of nitrogen and sulfur heteroatoms into inorganic ions, such as nitrate and ammonium, and sulfate ions, respectively [61].

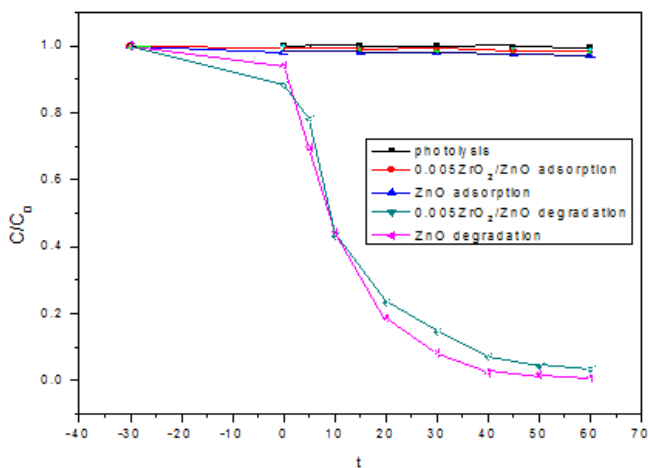


Figure 6: Photocatalytic degradation efficiency of ZnO and 0.005M ZrO₂/ZnO at 10ppm MB and 0.05g of ZnO and ZrO₂/ZnO

3.5.1. Effect of calcination temperatures on the photocatalytic activity:

The effect of calcination temperature on ZnO efficiency in degradation of MB is depicted in Fig.7. It can be noticed that the degradation efficiency increased with increasing calcination temperature from 400 °C to 500 °C and then

decreased greatly with further increase in calcination temperature to 600 °C. This deterioration in ZnO photodegradation efficiency at 600 °C is related to particle segregation. It is reported that photocatalytic activities of ZnO calcined at temperatures beyond 500 °C decreases rapidly due to increasing particle size and sintering of crystallites [20, 62]. This confirms that the particle size and crystallinity also plays an important role in deciding the catalyst performance along with surface area. ZnO catalyst calcined at 500 °C was found to be the most active catalyst for the photodegradation of MB under UV/Vis light. Thus, it is used as catalyst for optimizing key parameters of the photodegradation of MB under UV/Vis light.

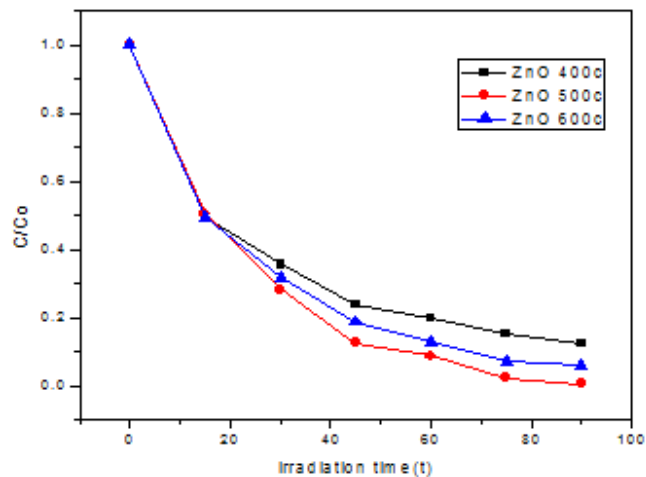


Figure 7: photocatalytic degradation curves of MB on ZnO treated under different temperatures

3.5.2 Effect of ZrO₂ doping concentration on photocatalytic properties of ZnO:

Fig.8 shows the photocatalytic degradation of MB on ZnO with different concentrations of ZrO₂. Decrease in photocatalytic efficiency by increasing concentration of ZrO₂ as a dopant is observed. This deficiency in photocatalytic activity arises from the fact that ZrO₂ has band gap around 5 eV and it cannot undergo direct band gap excitation at UV/Vis light [57]. The increase in particle size showed by XRD analysis (Fig.1) and TEM analysis (Fig.3) in ZrO₂ doped ZnO catalysts may be another reason for its photocatalytic deficiency.

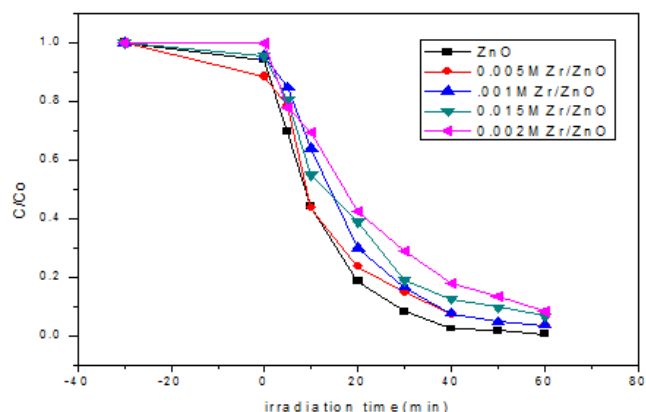


Figure 8: Photocatalytic degradation efficiency of ZnO and ZrO₂/ZnO at 10ppm MB and 0.05g of ZnO and ZrO₂/ZnO.

3.5.3 Effect of initial pH:

pH is an important factor that influences the photodegradation process of various pollutants. Effect of different values of pH (2.5, 7, 10) on the photocatalytic degradation of MB at constant concentration (10mg/L) and amount of $[ZnO]=1g/L$ is illustrated in Fig.9. Photodegradation efficiency of MB is increased by increasing pH values from pH 2.5–10. This variation is related to the change in electrostatic attraction or repulsion between dye molecules and catalyst. MB is a cationic dye and therefore the electrostatic attraction between the dye

molecules and catalyst surface is greatly improved at pH =10.

The observed enhancement in the degradation of MB at pH=10 can be attributed to the presence of excess hydroxyl groups on the catalyst surface. This results in the formation of more hydroxyl radicals (OH^\cdot) so electrostatic attraction will increase and then the photodegradation of MB increases [63]. The low photodegradation of MB in acidic medium (pH=2.5) is due to slight dissolution of ZnO and the catalyst surface will be protonated (have +Ve charge) so there will be electrostatic repulsion [64].

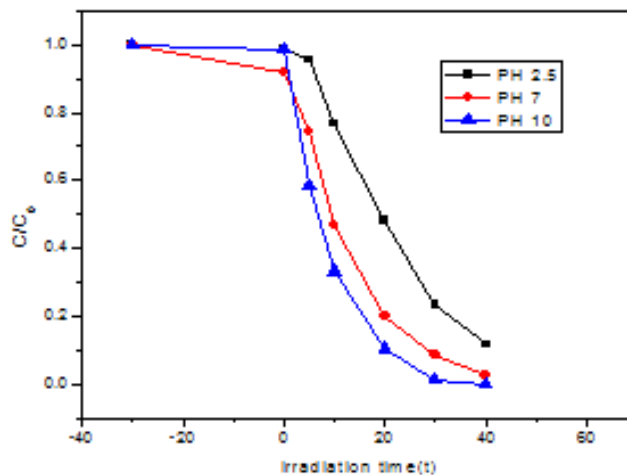


Figure 9: Photo degradation efficiency of MB at different pH values

3.5.4 Effect of initial concentration of MB

Dye concentration was investigated using initial concentrations of MB (10ppm, 20ppm, 50ppm and 100ppm), 0.05gm of catalyst and 50mL of dye solution at pH=10. The results illustrated in Fig.10(a, b), show that undoped ZnO had higher efficiency in photodegradation of MB at all concentrations.

Also it can be observed that the photodegradation efficiency decreased by increasing the dye concentration.

It is well known that photodegradation efficiency basically depends on the amount of hydroxyl radicals formed on the surface of the catalyst. As the concentration of dye increases, amount of dye adsorbed on the catalyst surface increases, consequently generation of hydroxyl radicals will be reduced. Furthermore, as the concentration of MB increases, the fewer photons reach the catalyst surface. As a result, the production of hydroxyl radicals that can attack the pollutants will decrease and photocatalytic efficiency decreases [65-66].

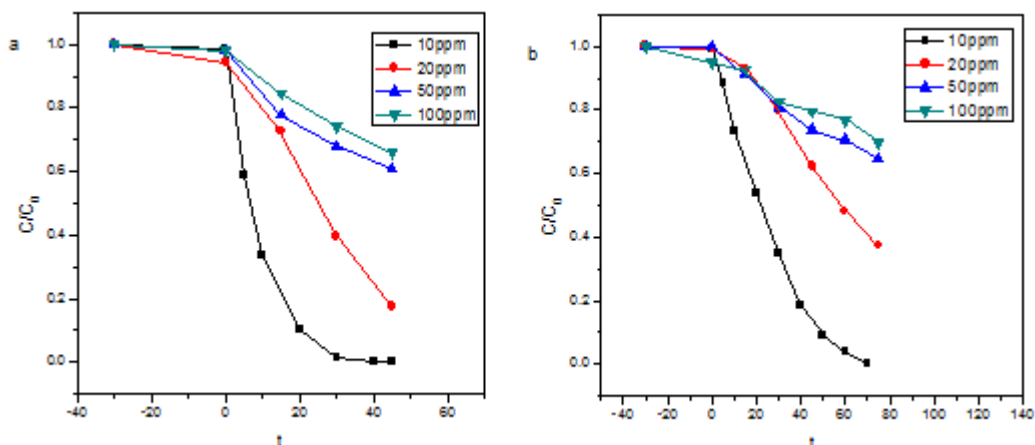


Figure 10: Effect of initial concentration of MB on the photodegradation efficiency of a) ZnO and b) 0.005M ZrO_2/ZnO under UV-Vis light

3.5.5. Kinetic studies of MB degradation using ZnO and 0.005 M ZrO₂/ZnO under UV-Vis light:

Kinetic studies of many organic pollutants have been modeled using Langmuir-Hinshelwood equation. This model is given by the equation below:

$$r = -\frac{dc}{dt} = K_{app}C$$

Where r is the degradation rate (mg/Lmin), the apparent constant of degradation (1/min), C is the concentration of MB dye (mg/L) at any time t.

The integration of this equation with limitation: C=C₀ for t = 0 leads to the following equation:

$$\ln \frac{C_0}{C} = K_{app}t$$

A straight line is obtained by plotting $\ln \frac{C_0}{C}$ vs. time, the slope of which upon linear regression equals the apparent first-order rate constant K_{app} [53].

The kinetics of decomposition of MB at different concentrations using ZnO and 0.005M ZrO₂/ZnO at pH = 10 is illustrated in Fig.11(a, b).The results show that the photocatalytic decomposition of MB by ZnO and 0.005 M ZrO₂/ZnO can be described by the first-order kinetic model. The plots of the concentration data gave a straight line. The correlation coefficient (R) for the fitted line and the rate constants (K_{app}) are calculated and their values are grouped in table2. R² is a measure of the strength and direction of the linear relationship between ln(C₀/C) and time (t). The more R² values approach 1, the more the relation will be linear indicating that the reaction is first order reaction.

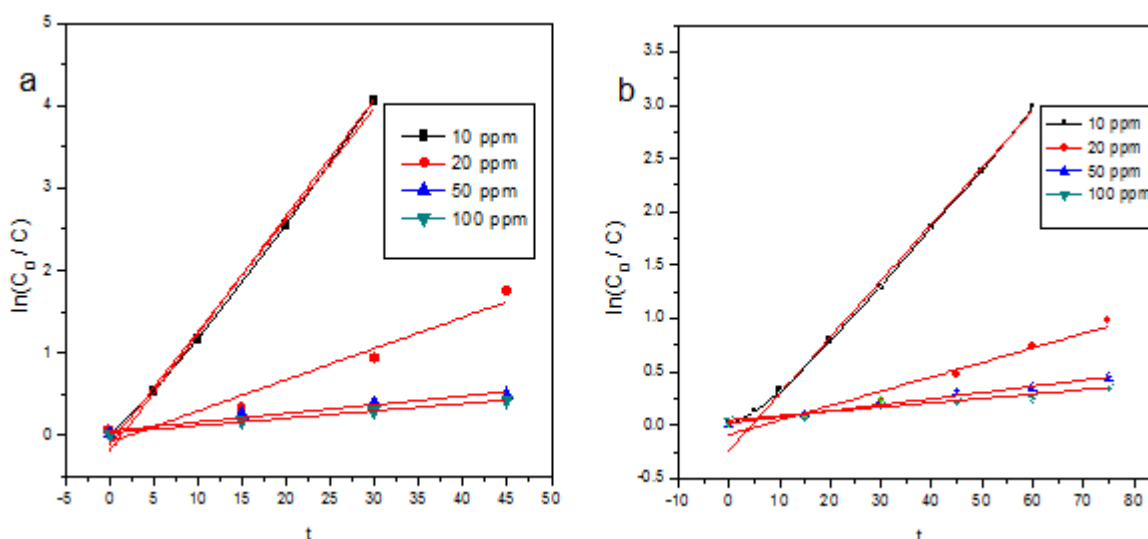


Figure 11: Kinetic fit for the degradation of MB with a) ZnO and b) 0.005M ZrO₂/ZnO

Table 2: Rate constants and correlation coefficients for catalytic photodecomposition of MB

C _i (mg/l)	ZnO		0.005M Zr/ZnO	
	K _{app}	R ²	K _{app}	R ²
10	0.1426	0.964	0.0531	0.956
20	0.0378	0.931	0.0136	0.957
50	0.0105	0.951	0.0058	0.981
100	0.0088	0.996	0.0041	0.958

Table 3: Shows the antibacterial activities of ZnO and ZrO₂ doped ZnO against tested organisms

No	Compound	S.Aureus (mg/ml)		C.Albicans (mg/ml)	
		Diameter of inhibition zone (in mm)	% activity index	Diameter of inhibition zone (in mm)	% activity index
1	ZnO	7	30.4	10	37.0
2	0.005MZrO ₂ /ZnO	8	34.8	15	55.5
3	0.01MZrO ₂ /ZnO	8	34.8	18	66.6
4	0.015MZrO ₂ /ZnO	11	47.8	16	59.2
5	0.02MZrO ₂ /ZnO	8	34.8	24	88.8
Ampicillin		23	100	NA	---
Colitrimazole		NA	---	27	100

• NA → No activity

4.6. Antibacterial activity:

In this work, bacterial strains of positive staphylococcus Aureus and negative candida Albicans were employed during the antibacterial test. ZnO and ZrO₂ doped ZnO samples exhibited a remarkable antibacterial activity against tested bacterial strains as shown in table 3. The antibacterial activity of a common standard antibiotic ampicillin and antifungal colitrimazole was also recorded using the same procedure at the same concentration and solvents to be considered as reference drug.

4. Conclusions

In recent work, ZnO and ZrO₂ doped ZnO nanoparticles have been prepared by sol-gel method. The X-ray diffraction (XRD) studies confirmed the formation of Wurtzite hexagonal phase of polycrystalline ZnO and ZrO₂ doped ZnO. SEM analysis showed that ZnO and ZrO₂ doped ZnO nano composites had a spherical shape. TEM analysis coincides with XRD analysis in that ZnO and ZrO₂ doped ZnO were in nano scale lower than 25 nm and increased in volume by increasing ZrO₂ content. Photocatalytic experiments showed that undoped ZnO is photocatalytically more active than ZrO₂ doped ZnO catalysts. However, ZrO₂ doped ZnO showed improvement in antimicrobial activity.

References

- [1] L. Ayed, K.Chaieb, A.Cheref, A.Bakhrouf, J.Microbiol. Biotechnol. 25 (2009) 705.
- [2] P.Borker, A.V.Salker, J.Mater. Sci.Engin. B133 (2006)55.
- [3] I.Udom, M.Ram, E.stefanakos, A.Hepp, J. Mater. sci. semicon. Process., 16(2013)2070
- [4] E. Forgacs, T.Cserhati, G.Oros, J. Environ. Intern. 30 (2004)953.
- [5] Z.He, C.Sun, S.Yang, Y.Ding, H.He, Z.Wang, J.Hazard.Maters., 162 (2009)1477.
- [6] L.Li, W.Dai, P.Yu, J.Zhao, Y.Qu, J. Chem. Technol. Biotechnol. , 84 (2009) 399.
- [7] H. Yang, H. Cheng, J.Separ.Purifi.Techn., 56 (2007)392.
- [8] C. Ma, Z. Zhou, H. Wei, Z. Yang, Z. Wang, Y. Zhang, J. Nanosc. Resea. Lett. 6(2011)536.
- [9] S. Rehman, R.Ullah, A.M.Butt, N.D.Gohar, J.Hazard. Maters. 170(2009)560.
- [10] S.H.S.Chan, T.Y.Wu, J.C.Juan, C.Y.Teh, J.chem. Technol. Biotechnol. , 86(2011)1130.
- [11] A. M. Ali, E. A. C.Emanuelsson, D.A.Patterson, J.Appl.Catal.B:Environ. 97(2010)168.
- [12] S.K. Pardeshi, A.B.Patil, J.Molec.Catal.A:Chem. 308 (2009)32.
- [13] M. Qamar, M.Muneer, J.Desalin. 249(2009)535.
- [14] J.Zhang, C.X.Pan, P.F.Fang, J.H.Wei, R.Xiong, J.ACSAppl.Maters.Interf., 4(2010)1173.
- [15] S. Sakhivel, B. Neppolian, M.V. Shankar, B. Arabindoo, M. Palanichamy, V.Murugesan, Sol. Energy Mater. Sol. Cells 77 (2003)65.
- [16] N.V. Kaneva, D.T.Dimitrov, C.D.Dushkin, Appl.Surf.Sci. 257 (2011) 8113.
- [17] E. Evgenidou, K.Fytianos, I.Poulios, J.Appl.Catal.B:Environ. 59(2005)81.
- [18] D. Lin, H.Wu, R.Zhang, W.Pan, J.Chem.Mater.21(2009) 3479.
- [19] F.D. Mai, C.S. Lu, C.W.Wu, C.H. Huang, J.Y. Chen, C.C. Chen, J.Sep. Purif. Technol.62 (2008) 423.
- [20] K.Hayat, M.A.Gondal, M.M.Khaled, S.Ahmed, A.M.Shemsi, J. Appl. Catal. A:Gen. 393(2011)122.
- [21] M.A.Behnajady, S.G.Moghaddam, N.Modirshahla, M.Shokri., J. Desalin. 249(2009) 1371.
- [22] X.Chen, Y.He, Q. Zhang, L.Li, D.Hu and T.Yin, J.Mater. Sci. 45 (2010) 953.
- [23] S.T. Christoskova, M. Stoyanova, J.Water Res. 35 (2001) 2073.
- [24] K.Gouvea, F.Wypych, S.G.Moraes, N. Duran, N. Nagata, P. PeraltaZamora, J.Chemosphere 40 (2000) 433.
- [25] S. Dindar, J. Icli, J. Photochem. Photobiol. A Chem. 140 (2001) 263.
- [26] M.A. Behnajady, N. Modirshahla, R. Hamzavi, J. Hazard. Mater. 133(2006) 226.
- [27] M.Fu, Y.Li, S.Wu, P.Lu, J.Liu, F.Dong, J.Appl.Sur.Sci 258(2011)1587.
- [28] O.Mekasuwandumrong, P.Pawinrat, P.Praserthdam, J.Panpranot, J.Chem.Eng. 164(2010)77
- [29] A.Dhir, N.T.Prakash, D.Sud, J.Desalin. 46(2012)196.
- [30] M. Ladanov, M.K.Ram, G.Matthews, A.Kumar, J.Langm. 27(2011) 9012.
- [31] K. Tanaka, K. Padermpole, T. Hisanaga, J.Water Resea. 34 (2000) 327.
- [32] A. Akyol, H.C. Yatmaz, M. Bayramoglu, J.Appl. Catal. B: Environ. 54 (2004)19.
- [33] R. Kavitha, S. Meghani, V. Jayaram, J.Mater. Sci. Eng. B 139 (2007) 134.

- [34] N. Daneshvar, D. Salari, A.R. Khataee, J. Photochem. Photobiol. A: Chem. 162 (2004) 317.
- [35] S.F. Chen, W. Zhao, W. Liu, S.J. Zhang, J. Appl. Surf. Sci. 255 (2008) 2478.
- [36] N. Sobana, M. Swaminathan, J. Separat. Puri. Techn. 56 (2007) 101.
- [37] Q. Wan, T.H. Wang, J.C. Zhao, J. Appl. Phys. Lett. 87 (2005) 083105.
- [38] C. Lizama, J. Freer, J. Baeza, H.D. Mansilla, J. Catal. Today 76 (2002) 235.
- [39] A. Shafaei, M. Nikazar, M. Arami, J. Desalin, 252 (2010) 8.
- [40] Y. Li, W. Xie, X. Hu, G. Shen, X. Zhou, Y. Xiang, X. Zhao, P. Fang, J. Langmuir 26 (1) (2010) 591.
- [41] R. Saravanan, V.K. Gupta, V. Narayanan, A. Stephen, J. Molec. Liq. 181 (2013) 133.
- [42] F. Tuomisto, K. Saarinen, K. Graszka, A. Mycielski, J. Phys. Status Solid. B 243 (2006) 794.
- [43] Y. Zheng, C. Chen, Y. Zhan, X. Lin, Q. Zheng, K. Wei, J. Zhu, Y. Zhu, J. Inorg. Chem. 46 (2007) 6675.
- [44] R.M. Sheetz, I. Ponomareva, E. Richter, A.N. Andriotis, M. Menon, J. Phys. Rev. B 80 (2009) 195314.
- [45] L. Cheng, Z.-Y. Zhang, J.-X. Shao, J. Acta Phys. Chim. Sin. 27 (2011) 846.
- [46] J.H. Luo, Q. Liu, L.N. Yang, Z.Z. Sun, Z.S. Li, J. Comp. Mater. Sci. 82 (2014) 70.
- [47] H. Tong, S. Ouyang, Y. Bi, N. Umezawa, M. Oshikiri, J. Adv. Mater. , 24 (2012) 229.
- [48] AN. Rao, B. Sivasankar, V. Sadasivam, J. Mol. Catal. A-Chem 306 (2009) 77.
- [49] M.A. Rauf, S.S. Ashraf, J. Hazard. Mater. 166 (2009) 6.
- [50] A. Akyol, M. Bayramoglu, J. Chem Eng. Process 47 (2008) 2150.
- [51] B.S. Rosales, I.H. de Lasa, A. Ortiz, M. Salaiques, J. Chem. Eng. Sci. 62 (2007) 5160.
- [52] B. Mokhlesi, J.B. Leikin, P. Murray, T.C. Corbridge, J. Chest 123 (2003) 897.
- [53] H. Benhebal, M. Chaib, T. Salmon, J. Geens, A. Leonard, S.D. Lambert, M. Crine, B. Heinrichs, J. Alex. Engin., 52 (2013) 517.
- [54] H. Benhebal, M. Chaib, C. Malengreaux, S.D. Lambert, A. Leonard, M. Crine, B. Heinrichs, J. Taiwan Inst. Chem. Eng. 45 (2014) 249.
- [55] S.A. El-Hakam, S.M. Hassan, A.I. Ahmed, S.M. El-Dadrawy, J. Americ. Sci., 7(3) (2011) 682.
- [56] Stylianakis, A. Kolocouris, G.B. Foscolos, E. Padalko, J. Neyts, D. Clerq, E. Bioorg, J. Med. Chem. Lett. 13 (2003) 1699.
- [57] E.D. Sherly, J.J. Vijaya, N.C.S. Selvam, L.J. Kennedy, J. Ceram. Int. 40 (2014) 5681.
- [58] M.M. Mezdrogina, E.Y. Danilevskii, R.V. Kuz'min, N.K. Poletaev, I.N. Trapeznikova, M.V. Chukichev, G.A. Bordovskii, A.V. Marchenko, M.V. Eremenko, J. Semicon., 44 (2010) 426.
- [59] J. Zhang, D. Gao, G. Yang, J. Zhang, Z. Shi, Z. Zhang, Z. Zhu, D. Xue, J. Nano Sc. Resea. Lett., 6 (2011) 487.
- [60] G. Sangeetha, S. Rajeshwari, R. Venckatesh, J. Mater. Resea. Bull. 46 (2011) 2560.
- [61] A. Houas, H. Lachheb, M. Ksibi, E. Elaloui, C. Guillard, J.M. Herrmann, J. Appl. Catal. B, 31 (2001) 145.
- [62] J.G. Yu, S.W. Liu, M.H. Zhou, J. Phys. Chem. C 112 (2008) 2050.
- [63] K. Vignesh, M. Rajarajan, A. Suganthia, J. Ind. Eng. Chem., 20 (2014) 3826.
- [64] Z. Yang, P. Zhang, Y. Ding, Y. Jiang, Z. Long, W. Dai, J. Mater. Res. Bull. 46 (2011) 1625.
- [65] S. Chakrabarti, B.K. Dutta, J. Hazard. Mater. 112 (2004) 269.
- [66] J. Wang, Y. Xie, Z. Zhang, J. Li, X. Chen, L. Zhang, R. Xu, X. Zhang, J. Sol. Mater., 93 (2009) 355